

**EFFECTS OF CLAY MODIFICATION AND  
COMPATIBILIZERS ON THE MECHANICAL,  
MORPHOLOGICAL, AND THERMAL  
PROPERTIES OF POLYAMIDE 6/  
POLYPROPYLENE NANOCOMPOSITES**

**KUSMONO**

**UNIVERSITI SAINS MALAYSIA**

**2008**

**EFFECTS OF CLAY MODIFICATION AND  
COMPATIBILIZERS ON THE MECHANICAL,  
MORPHOLOGICAL, AND THERMAL  
PROPERTIES OF POLYAMIDE 6/  
POLYPROPYLENE NANOCOMPOSITES**

**by**

**KUSMONO**

**Thesis submitted in fulfillment of the requirements  
for the degree of  
Doctoral of Philosophy**

**November 2008**

## ACKNOWLEDGMENT

Bismillaahirrahmaanirrahiim,

First and foremost, I would like to express my special gratitude to my supervisor Prof. Dr. Zainal Arifin Mohd Ishak for his valuable advice, encouragement, and constant dedication during my period of study. A sincere thanks is accorded to my co-supervisor Dr. Chow Wen Shyang for helpful discussions and insightful suggestions. Special thanks to Prof. Dr. Tsutomu Takeichi from Toyohashi University of Technology (TUT), Japan for his guidance, discussion, and extensive help with TEM measurements. I also wish to thank Dr. Rochmadi from Gadjah Mada University, Indonesia for his discussions and suggestions.

I would like to thank Dean Prof. Dr. Khairun Azizi BT. Mohd. Azizli, all lecturers, and administrative staffs for their kind cooperation and assistance. Thanks are also extended to technical staffs, En. Faisal, En. Rochman, En. Mohd. Hasan, En. Sahrir, En. Fitri, En. Rashid, En. Azam, and Mr. Segar for their invaluable assistance and technical support. The financial support and short-term study program at Department of Materials Science, TUT, Japan provided by AUN/SEED-Net Program JICA are greatly appreciated.

My sincere thanks are also extended to my friends of Indonesian students, namely Teguh, Sugeng, Fatur, Cahyo, Tedi, Triyogo, Rama, Zul, and Dibyo for their supports and friendship. Last but not least, I would like to convey my special thanks my parents, my lovely family, my loving wife Maryati and my sons Farras and Dzakwan who constantly supported and encouraged me.

## TABLE OF CONTENTS

<b>Acknowledgment</b>	ii
<b>Table of Contents</b>	iii
<b>List of Tables</b>	ix
<b>List of Figures</b>	xi
<b>List of Abbreviations</b>	xviii
<b>List of Symbols</b>	xix
<b>Abstrak</b>	xx
<b>Abstract</b>	xxii

### CHAPTER 1- INTRODUCTION

1.1	Introduction	1
1.2	Problem Statement	4
1.3	Objectives of Study	10

### CHAPTER 2 - LITERATURE REVIEW

2.1	Thermoplastics	11
	2.1.1 Polyamide 6 (PA6)	11
	2.1.2 Polypropylene (PP)	14
2.2	Polymer Blends	16
2.3	Compatibilization in Polymer Blends	17
	2.3.1 Maleic Anhydride Grafted Polypropylene (PP-g-MA)	19
	2.3.2 Maleic Anhydride Grafted Styrene-Ethylene-Butylene (SEBS-g-MA)	21
2.4	Thermoplastic Composites	22

2.5	Polymer Nanocomposites	23
2.6	Filler	24
	2.6.1 Layered Silicates	25
	2.6.2 Organoclay	27
2.7	Structures of Nanocomposites	29
2.8	Preparation Methods of Polymer Nanocomposites	31
2.9	Thermoplastic Nanocomposites	32
	2.9.1 Polyamide 6 Nanocomposites	32
	2.9.2 Polypropylene Nanocomposites	37
2.10	Characterization of Nanocomposites	40
	2.10.1 X-Ray Diffraction (XRD)	40
	2.10.2 Transmission Electron Microscopy (TEM)	41
2.11	Mechanical Properties and Fracture Behavior of Nanocomposites	42
2.12	Water Absorption	45
	2.12.1 Mechanism of Moisture Penetration	45
	2.12.2 Diffusion	46
	2.12.3 Water Absorption of Polyamide 6 Nanocomposites	47

### **CHAPTER 3 - EXPERIMENTAL**

3.1	Materials	50
	3.1.1 Thermoplastics	50
	3.1.1.1 Polyamide 6 (PA6)	50
	3.1.1.2 Polypropylene (PP)	50
	3.1.2 Organoclay	50

3.1.2.1	Commercial organoclay	50
3.1.2.2	Clay Modification	50
3.1.3	Compatibilizers	52
3.1.3.1	Maleic Anhydride Grafted Polypropylene (PP-g-MA)	52
3.1.3.2	Maleic Anydride Grafted Styrene Ethylene Butylene (SEBS-g-MA)	52
3.1.4	Designation and Composition of Samples	53
3.2	Sample Preparation	54
3.2.1	Compounding	54
3.2.2	Injection Molding	54
3.3	Sample Characterization	54
3.3.1	Melt Flow Index (MFI)	54
3.3.2	Fourier Transform Infra-Red Spectroscopy (FTIR) Analysis	54
3.3.3	X-Ray Diffraction (XRD)	55
3.3.4	Mechanical Properties	55
3.3.4.1	Tensile	55
3.3.4.2	Flexural	56
3.3.4.3	Izod Impact	56
3.3.4.4	Fracture Toughness	56
3.3.5	Morphology Studies	58
3.3.5.1	Transmission Electron Microscopy (TEM)	58
3.3.5.2	Field Emission Scanning Electron Microscopy (FESEM)	58
3.3.6	Thermal Properties	58
3.3.6.1	Differential Scanning Calorimetry (DSC)	58

3.3.6.2	Thermogravimetric Analysis (TGA)	59
3.3.6.3	Dynamic Mechanical Analysis (DMA)	59
3.3.6.4	Heat Distortion Temperature (HDT)	60
3.3.7	Water Absorption	60

## **CHAPTER 4 - RESULTS AND DISCUSSION**

4.1	Effect of Organoclay Loading on the PA6/PP Blend	62
4.1.1	Melt Flow Index (MFI)	62
4.1.2	Fourier Transform Infra-Red Spectroscopy (FTIR) Analysis	63
4.1.3	X-Ray Diffraction (XRD)	64
4.1.4	Mechanical Properties	65
4.1.4.1	Tensile Properties	65
4.1.4.2	Flexural Properties	69
4.1.4.3	Izod Impact Properties	70
4.1.4.4	Fracture Toughness	71
4.1.5	Morphology Studies	73
4.1.6	Thermal Properties	78
4.1.6.1	Differential Scanning Calorimetry (DSC)	78
4.1.6.2	Thermogravimetric Analysis (TGA)	82
4.2	Effect of Compatibilizers on the PA6/PP/Organoclay Nanocomposites	84
4.2.1	Melt Flow Index (MFI)	84
4.2.2	Fourier Transform Infra-Red Spectroscopy (FTIR) Analysis	86
4.2.3	X-Ray Diffraction (XRD)	88
4.2.4	Mechanical Properties	92
4.2.5	Morphology Studies	104

4.2.6	Thermal Properties	109
4.2.6.1	Differential Scanning Calorimetry (DSC)	109
4.2.6.2	Thermogravimetric Analysis (TGA)	117
4.3	Effects of Clay Modification and Compatibilizers on the PA6/PP/Organoclay Nanocomposites	121
4.3.1	Melt Flow Index (MFI)	121
4.3.2	Fourier Transform Infra-Red Spectroscopy (FTIR) Analysis	123
4.3.3	X-Ray Diffraction (XRD)	124
4.3.4	Mechanical Properties	132
4.3.4.1	Tensile Properties	132
4.3.4.2	Flexural Properties	143
4.3.4.3	Izod Impact Properties	148
4.3.4.4	Fracture Toughness	152
4.3.5	Morphology Studies	157
4.3.6	Thermal Properties	163
4.3.6.1	Differential Scanning Calorimetry (DSC)	163
4.3.6.2	Thermogravimetric Analysis (TGA)	171
4.3.6.3	Dynamic Mechanical Analysis (DMA)	173
4.3.6.4	Heat Distortion Temperature (HDT)	184
4.4	Effect of Testing Speed	185
4.4.1	Mechanical Properties	185
4.4.1.1	Tensile Properties	185
4.4.1.2	Fracture Toughness	196
4.4.2	Morphology Studies	202
4.5	Water Absorption	211

4.5.1	Kinetics of Water Absorption	211
4.5.2	Mechanical Properties	217
4.5.3	Morphology Studies	222

## **CHAPTER 5 - CONCLUSIONS AND SUGGESTIONS FOR FUTURE WORKS**

5.1	Conclusions	227
5.2	Suggestions for Future Works	230

<b>BIBLIOGRAPHY</b>		231
---------------------	--	-----

## **APPENDICES**

A.1	Paper 1 (Abstract) EUROPEAN POLYMER JOURNAL	245
A.2	Paper 2 (Abstract ) eXPRESS Polymer Letters	247
A.3	Paper 3 (Abstract ) COMPOSITES PART A: APPLIED SCIENCE AND MANUFACTURING	249
A.4	Paper 4 (Abstract ) POLYMER COMPOSITES	251
A.5	Conference Proceeding 1 (FWS VI), Malaysia	253
A.6	Conference Proceeding 2 (MAMIP), Malaysia	254
A.7	Conference Proceeding 3 (ICCS) International, Indonesia	255
A.8	Conference Proceeding 4 (FWS X), Malaysia	256
A.9	Conference Proceeding 5 (NSPM), Malaysia	257
A.10	Conference Proceeding 6 (PPS-24) International, Salerno Italy	258

## LIST OF TABLES

		Page
Table 2.1	Polymer blends with compatibilizers	19
Table 2.2	Forms of various fillers [Charrier, 1990]	24
Table 2.3	Chemical formula and characteristic parameter of commonly 2:1 phyllosilicates [Sinhay Ray and Okamoto, 2003]	26
Table 3.1	The characteristic of alkyl ammonium salts used for clay modification	51
Table 3.2	Designation and composition of samples using commercial organoclay	53
Table 3.3	Designation and composition of samples using clay modification	53
Table 4.1	Thermal characteristics of PA6/PP blend and its nanocomposites	79
Table 4.2	Effects of compatibilizers on the MFI values of PA6/PP blends and its nanocomposites	86
Table 4.3	Mechanical properties of PA6/PP blends and its nanocomposites with and without PP-g-MA	94
Table 4.4	Mechanical properties of PA6/PP blends and its nanocomposites with and without SEBS-g-MA	97
Table 4.5	DSC results of PA6/PP blends and its nanocomposites with and without PP-g-MA	112
Table 4.6	DSC results of PA6/PP blends and its nanocomposites with and without SEBS-g-MA	116
Table 4.7	TGA results of PA6/PP blends and its nanocomposites compatibilized with PP-g-MA and SEBS-g-MA	120
Table 4.8	Effects of clay modification and compatibilizers on the MFI values of PA6/PP/OMMT nanocomposites	122
Table 4.9	Basal spacing ( $d_{001}$ ) of Na-MMT and MMT modified with various organic modifiers (OMMT)	126
Table 4.10	DSC results of the uncompatibilized and compatibilized PA6/PP/OMMT nanocomposites	170

Table 4.11	$T_g$ and HDT results of PA6/PP blend and its nanocomposites	183
Table 4.12	Equilibrium water content, $M_m$ and diffusivity, $D$ of PA6/PP/OMMT nanocomposites	211
Table 4.13	Tensile properties of PA6/PP/OMMT nanocomposites in control, wet, and re-dried states	221

## LIST OF FIGURES

	Page	
Figure 2.1	Synthesis of nylon 6,6 [Painter and Coleman, 1994]	13
Figure 2.2	Typical ring-opening polymerization of caprolactam [Painter and Coleman, 1994]	14
Figure 2.3	Polymerization of propylene to polypropylene [Baker and Mead, 2002]	15
Figure 2.4	Structure of 2:1 phyllosilicates [Sinha Ray and Okamoto, 2003]	26
Figure 2.5	Possible orientation of alkylammonium ions in the galleries of layered silicates [LeBaron et al., 1999]	28
Figure 2.6	Schematic representation of a cation-exchange reaction between the silicate and an alkylammonium salt [Zanetti et al., 2000]	29
Figure 2.7	Scheme of different types of composite arising from the interaction of layered silicates and polymers: (a) phase separated microcomposite; (b) intercalated nanocomposite and (c) exfoliated nanocomposite [Alexandre and Dubois, 2000]	30
Figure 2.8	Typical XRD patterns for polymer-layered silicates nanocomposites [Giannelis et al., 1999]	41
Figure 2.9	TEM images of exfoliated (a) and intercalated (b) nanocomposites [Liu et al., 2003]	42
Figure 3.1	Geometry of the SEN-3PB specimen	57
Figure 4.1	Effect of organoclay content on the MFI value of PA6/PP blend	62
Figure 4.2	FTIR spectra of organoclay, PA6/PP blend, and its nanocomposite	64
Figure 4.3	XRD patterns of organoclay, PA6/PP blend, and its nanocomposites	65
Figure 4.4	Effect of organoclay content on the tensile modulus and strength of PA6/PP/organoclay nanocomposites	66

Figure 4.5	Effect of organoclay content on the elongation at break of PA6/PP/organoclay nanocomposites	68
Figure 4.6	Effect of organoclay content on the flexural modulus and strength of PA6/PP/organoclay nanocomposites	70
Figure 4.7	Effect of organoclay content on the Izod impact strength of the PA6/PP/organoclay nanocomposites	71
Figure 4.8	Effect of organoclay content on the fracture toughness of the PA6/PP/organoclay nanocomposites	73
Figure 4.9	TEM image of PA6/PP/organoclay nanocomposite filled with 4 phr of organoclay	74
Figure 4.10	TEM image of PA6/PP/organoclay nanocomposite filled with 10 phr of organoclay	75
Figure 4.11	SEM micrographs taken from tensile fractured surface of: (a). PA6/PP blend (b). Nanocomposite filled with 4 phr of organoclay	77
Figure 4.12	DSC heating scans of PA6/PP blend and its nanocomposites	81
Figure 4.13	DSC cooling scans of PA6/PP blend and its nanocomposites	82
Figure 4.14	TGA curves of PA6/PP blend and its nanocomposite. The insert shows the zoom of the oval portion indicating weight (%) as a function of temperature (°C).	84
Figure 4.15	FT-IR spectra of PA6/PP blends and PA6/PP/4C-MMT nanocomposite with and without PP-g-MA and SEBS-g-MA	88
Figure 4.16	XRD patterns of organoclay, PA6/PP blends, and PA6/PP/4C-MMT nanocomposite with and without PP-g-MA	90
Figure 4.17	XRD patterns of organoclay, PA6/PP blends, and PA6/PP/4C-MMT nanocomposite with and without SEBS-g-MA	92
Figure 4.18	Possible interaction between PP, SEBS-g-MA, and PA6	102
Figure 4.19	Possible interaction between PP, SEBS-g-PA6, and organoclay	103
Figure 4.20	TEM micrograph taken from the PA6/PP/organoclay nanocomposite compatibilized with 5 phr of PP-g-MA	105

Figure 4.21	TEM micrograph taken from the PA6/PP/organoclay nanocomposite compatibilized with 5 phr of SEBS-g-MA	106
Figure 4.22	SEM micrograph of tensile fractured surface of the PP-g-MA compatibilized PA6/PP/organoclay nanocomposite (PA6/PP/5P/4C-MMT)	107
Figure 4.23	SEM micrograph of tensile fractured surface of the SEBS-g-MA compatibilized PA6/PP nanocomposite (PA6/PP/5S/4C-MMT)	109
Figure 4.24	DSC heating scans of PA6/PP blends and its nanocomposites with and without PP-g-MA	111
Figure 4.25	DSC cooling scans of PA6/PP blends and its nanocomposites with and without PP-g-MA	112
Figure 4.26	DSC heating scans of PA6/PP blends and its nanocomposites with and without SEBS-g-MA	115
Figure 4.27	DSC heating scans of PA6/PP blends and its nanocomposites with and without SEBS-g-MA	116
Figure 4.28	TGA curves of PA6/PP blends and its nanocomposites with and without PP-g-MA. The insert shows the zoom of the oval portion indicating weight (%) as a function of temperature (°C)	118
Figure 4.29	TGA curves of PA6/PP blends and its nanocomposites with and without SEBS-g-MA. The insert shows the zoom of the oval portion indicating weight (%) as a function of temperature (°C)	120
Figure 4.30	FT-IR spectra of Na-MMT and OMMT	124
Figure 4.31	XRD patterns of Na-MMT and OMMT	126
Figure 4.32	XRD patterns of PA6/PP blend, PA6/PP/4Na-MMT, and PA6/PP/OMMT nanocomposite	128
Figure 4.33	XRD patterns of PP-g-MA compatibilized PA6/PP/OMMT nanocomposites	130
Figure 4.34	XRD patterns of SEBS-g-MA compatibilized PA6/PP/OMMT nanocomposites	132
Figure 4.35	Effect of clay modification on the tensile modulus and strength of PA6/PP/OMMT nanocomposites	134

Figure 4.36	Effect of clay modification on the elongation at break of PA6/PP/OMMT nanocomposites	135
Figure 4.37	Effect of PP-g-MA on the tensile modulus of PA6/PP/OMMT nanocomposites	137
Figure 4.38	Effect of PP-g-MA on the tensile strength of PA6/PP/OMMT nanocomposites	138
Figure 4.39	Effect of PP-g-MA on the elongation at break of PA6/PP/OMMT nanocomposites	139
Figure 4.40	Effect of SEBS-g-MA on the tensile modulus of PA6/PP/OMMT nanocomposites	140
Figure 4.41	Effect of SEBS-g-MA on the tensile strength of PA6/PP/OMMT nanocomposites	141
Figure 4.42	Effect of SEBS-g-MA on the elongation at break of PA6/PP/OMMT nanocomposites	142
Figure 4.43	Effect of clay modification on the flexural modulus and strength of PA6/PP/OMMT nanocomposites	144
Figure 4.44	Effect of PP-g-MA on the flexural modulus of PA6/PP/OMMT nanocomposite	145
Figure 4.45	Effect of PP-g-MA on the flexural strength of PA6/PP/OMMT nanocomposites	146
Figure 4.46	Effect of SEBS-g-MA on the flexural modulus of PA6/PP/OMMT nanocomposites	147
Figure 4.47	Effect of SEBS-g-MA on the flexural strength of PA6/PP/OMMT nanocomposites	147
Figure 4.48	Effect of clay modification on the Izod impact strength of PA6/PP/OMMT nanocomposites	149
Figure 4.49	Effect of PP-g-MA on the Izod impact strength of PA6/PP/OMMT nanocomposites	150
Figure 4.50	Effect of SEBS-g-MA on the Izod impact strength of PA6/PP/OMMT nanocomposites	152
Figure 4.51	Effect of clay modification on the fracture toughness of PA6/PP/OMMT nanocomposites	154

Figure 4.52	Effect of PP-g-MA on the fracture toughness of PA6/PP/OMMT nanocomposites	155
Figure 4.53	Effect of SEBS-g-MA on the fracture toughness of PA6/PP/OMMT nanocomposites	157
Figure 4.54	TEM image of PA6/PP/4Na-MMT composite	158
Figure 4.55	TEM image of PA6/PP/4D-MMT nanocomposite	158
Figure 4.56	TEM image of PA6/PP/4S-MMT nanocomposite	159
Figure 4.57	TEM images of PP-g-MA compatibilized PA6/PP/4D-MMT nanocomposite at different magnifications: a. 10,000X    b. 40,000X    c. 100,000X	162
Figure 4.58	TEM image of SEBS-g-MA compatibilized PA6/PP/4S-MMT nanocomposite	163
Figure 4.59	DSC heating scans of uncompatibilized and PP-g-MA compatibilized PA6/PP/OMMT nanocomposites	166
Figure 4.60	DSC cooling scans of uncompatibilized and PP-g-MA compatibilized PA6/PP/OMMT nanocomposites	167
Figure 4.61	DSC heating scans of uncompatibilized and SEBS-g-MA compatibilized PA6/PP/OMMT nanocomposites	169
Figure 4.62	DSC cooling scans of uncompatibilized and SEBS-g-MA compatibilized PA6/PP/OMMT nanocomposites	170
Figure 4.63	TGA curves of Na-MMT and OMMT	172
Figure 4.64	DTG curves of Na-MMT and OMMT	173
Figure 4.65	Storage modulus as function of temperature for PA6/PP blend and its nanocomposites	176
Figure 4.66	Tan $\delta$ as function of temperature for PA6/PP blend and its nanocomposites	177
Figure 4.67	Effect of PP-g-MA on the storage modulus as function of temperature for PA6/PP/OMMT nanocomposites	179
Figure 4.68	Effect of PP-g-MA on the tan $\delta$ as function of temperature for PA6/PP/OMMT nanocomposites	180
Figure 4.69	Effect of SEBS-g-MA on the storage modulus as function of temperature for PA6/PP/OMMT nanocomposites	182

Figure 4.70	Effect of SEBS-g-MA on the $\tan \delta$ as function of temperature for PA6/PP/OMMT nanocomposites	183
Figure 4.71	Effect of testing speed on the tensile modulus of PA6/PP blend and its nanocomposites	186
Figure 4.72	Effect of testing speed on the tensile strength of PA6/PP blend and its nanocomposites	187
Figure 4.73	Effect of testing speed on the elongation at break of PA6/PP/OMMT nanocomposites	189
Figure 4.74	Effect of testing speed on the tensile modulus of PP-g-MA compatibilized PA6/PP/OMMT nanocomposites	190
Figure 4.75	Effect of testing speed on the tensile strength of PP-g-MA compatibilized PA6/PP/OMMT nanocomposites	191
Figure 4.76	Effect of testing speed on the elongation at break of PP-g-MA compatibilized PA6/PP/OMMT nanocomposites	192
Figure 4.77	Effect of testing speed on the tensile modulus of SEBS-g-MA compatibilized PA6/PP/OMMT nanocomposites	193
Figure 4.78	Effect of testing speed on the tensile strength of SEBS-g-MA compatibilized PA6/PP/OMMT nanocomposites	194
Figure 4.79	Effect of testing speed on the elongation at break of SEBS-g-MA compatibilized PA6/PP/OMMT nanocomposites	196
Figure 4.80	Effect of testing speed on the fracture toughness of PA6/PP blend and its nanocomposites	198
Figure 4.81	Effect of testing speed on the fracture toughness of PP-g-MA compatibilized PA6/PP/OMMT nanocomposites	199
Figure 4.82	Effect of testing speed on the fracture toughness of SEBS-g-MA compatibilized PA6/PP/OMMT nanocomposites	201
Figure 4.83	SEM micrographs of SEN-3PB fracture surface of the PA6/PP blend at different testing speeds. (a) 1 mm/min; (b) 500 mm/min	202
Figure 4.84	SEM micrographs of SEN-3PB fracture surface of the PA6/PP/4A-MMT nanocomposite at different testing speeds. (a) 1 mm/min; (b) 500 mm/min	203

Figure 4.85	SEM micrographs of SEN-3PB fracture surface of the PA6/PP/4C-MMT nanocomposite at different testing speeds. (a) 1 mm/min; (b) 500 mm/min	204
Figure 4.86	SEM micrographs of SEN-3PB fracture surface of the PP-g-MA compatibilized PA6/PP/4A-MMT nanocomposite at different testing speeds. (a) 1 mm/min; (b) 500 mm/min	206
Figure 4.87	SEM micrographs of SEN-3PB fracture surface of the PP-g-MA compatibilized PA6/PP/4C-MMT nanocomposite at different testing speeds. (a) 1 mm/min; (b) 500 mm/min	207
Figure 4.88	SEM micrographs of SEN-3PB fracture surface of the SEBS-g-MA compatibilized PA6/PP/4A-MMT nanocomposite at different testing speeds. (a) 1 mm/min; (b) 500 mm/min	209
Figure 4.89	SEM micrographs of SEN-3PB fracture surface of the SEBS-g-MA compatibilized PA6/PP/4C-MMT nanocomposite at different testing speeds. (a) 1 mm/min; (b) 500 mm/min	210
Figure 4.90	Water absorption curves of PA6/PP/OMMT nanocomposites	212
Figure 4.91	Water absorption curves of PP-g-MA compatibilized PA6/PP/OMMT nanocomposites	213
Figure 4.92	Water absorption curves of SEBS-g-MA compatibilized PA6/PP/OMMT nanocomposites	214
Figure 4.93	SEM micrographs of the tensile fractured surface of PA6/PP blend. (a) Control; (b) On water absorption	222
Figure 4.94	SEM micrographs of the tensile fractured surface of PA6/PP/4C-MMT nanocomposites. (a) Control; (b) On water absorption	223
Figure 4.95	SEM micrographs of the tensile fractured surface of PP-g-MA compatibilized PA6/PP/4C-MMT nanocomposites. (a) Control; (b) On water absorption	225
Figure 4.96	SEM micrographs of the tensile fractured surface of SEBS-g-MA compatibilized PA6/PP/4C-MMT nanocomposite. (a) Control; (b) On water absorption	226

## LIST OF ABBREVIATIONS

AFM	Atomic Force Microscopy
DMA	Dynamic Mechanical Analysis
DSC	Differential Scanning Calorimetry
EPDM	Ethylene-Propylene-Diene Rubber
EPR-g-MA	Maleic Anhydride Grafted Ethylene-Propylene-Rubber
FESEM	Field Emission Scanning Electron Microscopy
FT-IR	Fourier-Transform Infra-Red Spectroscopy
HDT	Heat Distortion Temperature
LDPE	Low Density Polyethylene
PBT	Poly(butylenes terephthalate)
PC	Polycarbonate
PS	Polystyrene
PE-g-MA	Maleic Anhydride Grafted Polyethylene
PE-g-PEO	Poly(ethylene-graft-ethylene oxide)s
PP-g-MA	Maleic Anhydride Grafted Polypropylene
PP-g-MA-co-POP	Poly(oxypropylene)-amide grafted polypropylene
POE-g-MA	Maleic Anhydride Grafted Polyethylene-Octene Elastomer
SBS	Styrene-Butylene-Styrene
SEBS-g-MA	Maleic Anhydride Grafted Styrene-Ethylene/Butylene-Styrene
SMA	Styrene grafted Maleic Anhydride
TEM	Transmission Electron Microscopy
TGA	Thermogravimetric Analysis
XRD	X-Ray Diffraction

## LIST OF SYMBOLS

$d$	Spacing between diffraction lattice plane (interspacing)
$\theta$	Diffraction angle
$\lambda$	Wave length
$K_{IC}$	Fracture toughness
$P$	Maximum load
$S$	Length of the span
$B$	Thickness of the specimen for SEN-3PB specimen
$a$	Total notch length
$T_m$	Melting temperature
$T_c$	Crystallization temperature
$X_C$	Degree of crystallinity
$\Delta H$	Heat of fusion for sample
$\Delta H_f^0$	Heat of fusion for 100% crystalline
$E'$	Storage modulus
$\tan \delta$	Loss factor
$W_d$	Weight of dry sample
$W_w$	Weight of samples after exposed to in deionized water
$M_t$	Percentage weight at time t
$M_m$	percentage equilibrium or maximum water absorption
$D$	Diffusion coefficient or diffusivity
$T_g$	Glass transition temperature

**KESAN PENGUBAHSUAIAN TANAH LIAT DAN AGEN PENSERASI KE  
ATAS SIFAT-SIFAT MEKANIK, MORFOLOGI, DAN TERMA BAGI  
NANOKOMPOSIT POLIAMIDA 6/POLIPROPILENA**

**ABSTRAK**

Nanokomposit yang mengandungi gaulan poliamida 6 (PA6)/polipropilena (PP) PA6/PP (70/30) dan organo-tanah liat (0-10 phr) telah disediakan menggunakan penyebatan leburan. Sifat mekanik nanokomposit telah diukur melalui spesimen pengacuanan suntikan menggunakan ujian tensil, ujian fleksural, ujian hentaman Izod dan ujian keliatan retak. Kekakuan dan kekuatan optimum telah diperhatikan pada 4 phr organo-tanah liat. Morfologi nanokomposit telah diperhatikan dengan menggunakan mikroskop elektron imbasan (SEM), mikroskop elektron transmisi (TEM), dan penyerakan sinar-x (XRD). Telah diperhatikan bahawa organo-tanah liat telah didapati tereksfoliasi dengan baik dalam fasa PA6. Polipropilena tercantum maleik anhidrida (PP-g-MA) dan stirena-etilena/butilena-stirena tercantum maleik anhidrida (SEBS-g-MA) telah digunakan untuk menserasikan sistem komposit PA6/PP/organo-tanah liat. Kajian mikroskop elektron imbasan (SEM) menunjukkan bahawa kehadiran pengserasi telah menurunkan saiz domain fasa PP. Kekakuan, kekuatan dan keliatan nanokomposit PA6/PP telah meningkat dengan kehadiran pengserasi PP-g-MA yang disebabkan oleh kesan pengserasi PP-g-MA. Dalam erti kata lain, penambahan SEBS-g-MA mengurangkan kekakuan dan kekuatan walau bagaimanapun ia telah meningkatkan keliatan nanokomposit PA6/PP. Keputusan XRD dan TEM menunjukkan pembentukan struktur tereksfoliasi bagi nanokomposit PA6/PP yang diserasikan oleh kedua-dua PP-g-MA dan SEBS-g-MA. Pengubahsuaian natrium montmorillonit (Na-MMT) dengan 3 jenis garam ammonium alkil iaitu dodesilamina, asid 12-aminolaurik, dan stearilamina melalui tindak balas penukar ion telah berjaya dihasilkan. Disamping itu, organo-tanah liat

komersil (C-MMT) juga digunakan di dalam penyelidikan ini. Pengubahsuaian tanah liat telah meningkatkan kekakuan dan kekuatan namun mengurangkan kemuluran dan keliatan bagi matriks PA6/PP. Nanokomposit PA6/PP yang mengandungi montmorillonit terubahsuai stearilamina (S-MMT) mempamerkan kekakuan dan kekuatan yang paling tinggi diikuti oleh nanokomposit yang mengandungi organo-tanah liat komersil (C-MMT), montmorillonit terubahsuai asid 12-aminolaurik (A-MMT), dan seterusnya montmorillonit terubahsuai dodesilamina (D-MMT). Pengubahsuaian tanah liat yang terbaik S-MMT mungkin disebabkan oleh rantai alkil S-MMT yang lebih panjang yang kemudian memberi kesan kepada jarak basal yang lebih jauh dan eksfoliasi lapisan silikat yang lebih baik. Penambahan kedua-dua PP-g-MA and SEBS-g-MA menyebabkan peningkatan kekuatan nanokomposit PA6/PP yang jelas. Analisis mekanik dinamik (DMA) dan suhu pengerotan haba (HDT) telah digunakan untuk mengkaji sifat mekanik dinamik dan kestabilan termal bagi nanokomposit PA6/PP. Modulus simpanan dan HDT bagi matrik PA6/PP telah meningkat dengan signifikan dengan kehadiran pengubahsuaian tanah liat. Penambahan PP-g-MA dan SEBS-g-MA kepada nanokomposit PA6/PP telah menurunkan suhu peralihan kaca ( $T_g$ ) dan HDT. Keliatan retak ( $K_{IC}$ ) bagi semua nanokomposit PA6/PP yang diserasikan dengan SEBS-g-MA meningkat dengan peningkatan halaju pengujian. Kinetik penyerapan air bagi nanokomposit PA6/PP menepati hukum Fick. Didapati bahawa nanokomposit PA6/PP menunjukkan nilai kandungan kelembapan keseimbangan ( $M_m$ ) dan koefisien pembauran ( $D$ ) yang lebih tinggi berbanding matrik PA6/PP. Modulus tensil dan kekuatan tensil menurun dengan penyerapan air tetapi sebaliknya keliatan tensil meningkat. Penambahan pengserasi PP-g-MA dan SEBS-g-MA telah meningkatkan rintangan penyerapan air, kemampuan penahanan, dan sifat pemulihan bagi nanokomposit PA6/PP.

# **EFFECTS OF CLAY MODIFICATION AND COMPATIBILIZERS ON THE MECHANICAL, MORPHOLOGICAL, AND THERMAL PROPERTIES OF POLYAMIDE 6/POLYPROPYLENE NANOCOMPOSITES**

## **ABSTRACT**

Nanocomposites containing polyamide 6 (PA6)/polypropylene (PP) PA6/PP (70/30) blend and organoclay (0-10 phr) were prepared by melt compounding. The mechanical properties of the nanocomposites were determined on injection-molded specimens using tensile, flexural, Izod impact, and fracture toughness tests. The optimum stiffness and strength was observed at 4 phr of organoclay. The morphology of the nanocomposites was investigated by scanning electron microscopy (SEM), transmission electron microscopy (TEM), and x-ray diffraction (XRD). It was observed that the organoclay was well exfoliated and preferentially embedded in the PA6 phase. Furthermore, maleic anhydride grafted polypropylene (PP-g-MA) and maleic anhydride grafted styrene-ethylene/butylene-styrene (SEBS-g-MA) were used to compatibilize the PA6/PP/organoclay systems. SEM examination indicated that the presence of compatibilizers has reduced the domain size of PP phase. The stiffness, strength, and toughness of PA6/PP nanocomposites were improved in the presence of PP-g-MA compatibilizer due to the compatibilizing effect of PP-g-MA. On other hand, the addition of SEBS-g-MA has reduced the stiffness and strength; however improved the toughness of PA6/PP nanocomposites. XRD and TEM results revealed the formation of exfoliated structure in both PP-g-MA and SEBS-g-MA compatibilized PA6/PP nanocomposites. The modification of sodium montmorillonite (Na-MMT) with three different types of alkyl ammonium salts, namely dodecylamine, 12-aminolauric acid, and stearylamine through cation exchange reaction has been successfully performed. Besides that, the commercial

organoclay (C-MMT) was also used in this study. The clay modification has increased stiffness and strength at the expense of ductility and toughness of PA6/PP matrix. The PA6/PP nanocomposite containing stearylamine modified montmorillonite (S-MMT) showed the highest stiffness and strength followed by the nanocomposites containing commercial organoclay (C-MMT), 12 aminolauric acid modified montmorillonite (A-MMT), and then dodecylamine modified montmorillonite (D-MMT). The best type of clay modification of S-MMT may be attributed to the longer alkyl chain of S-MMT which then resulted in higher basal spacing as well as better exfoliation of silicate layers. Furthermore, the incorporation of both PP-g-MA and SEBS-g-MA has led to a significant increase in strength of the PA6/PP nanocomposites. Dynamic mechanical analysis (DMA) and heat distortion temperature (HDT) were used to study dynamic mechanical properties and thermal stability of the PA6/PP nanocomposites, respectively. The storage modulus and HDT of PA6/PP matrix significantly increased in the presence of clay modification. The addition of both PP-g-MA and SEBS-g-MA into the PA6/PP nanocomposites has decreased the glass transition temperature ( $T_g$ ) and HDT values. The fracture toughness ( $K_{IC}$ ) of all SEBS-g-MA compatibilized PA6/PP nanocomposites significantly enhanced with increasing testing speed. The kinetics of water absorption of the PA6/PP nanocomposites conforms to Fick law. It was found that the PA6/PP nanocomposites exhibited higher  $M_m$  and  $D$  values than the PA6/PP blend. Both the tensile modulus and strength deteriorated drastically upon water absorption but the ductility improved. The addition of both PP-g-MA and SEBS-g-MA compatibilizers has improved the resistance of water absorption, retention-ability, and recovery properties of the PA6/PP nanocomposites.

# CHAPTER 1

## INTRODUCTION

### 1.1 Introduction

In recent years, polymer/clay nanocomposites (PCNs) have attracted significant academic and industrial interest. This interest stems from the fact that nano-sized-layer-filled polymers can exhibit dramatic improvements in mechanical and thermal properties at low clay contents because of the strong synergistic effects between the polymer and the silicate platelets on both the molecular or nanometric scale [Sinha Ray and Okamoto, 2003]. PCNs are new class of composite materials, in which clay as layered silicate is dispersed in nanoscale size in a polymer matrix. The potential properties enhancements of PCNs have led to increased application in various fields such as the automobile industry (exterior and interior body parts and fuel tanks), packaging industry (bottles, containers, and plastic films), electronic industry (packaging material and exterior parts of electronic devices), coating industry (paints, wire enamel coatings, etc), and aerospace industry (body parts of airplane and exterior surface coatings). PCNs can be prepared by four different methods: exfoliation-adsorption, in situ intercalative polymerization, melt intercalation, and template synthesis [Alexandre and Dubois, 2000]. Among them, melt intercalation (melt compounding) is the most industrially valuable because of its environmentally benign character, its versatility, and its compatibility with current polymer processing techniques such as extrusion and injection molding [Vaia et al., 1995].

The most commonly used clay is the smectite group mineral such as montmorillonite (MMT), which belongs to the general family of 2:1 layered silicates. Its structure consists of two fused silica tetrahedral sheets sandwiching an edge-

shared octahedral sheet of either aluminum or magnesium hydroxide [Whittingham and Jacobson, 1982]. The use of layered silicate as reinforcement is hindered because of the preferred face-to-face stacking of nanolayers in agglomerated tactoids and intrinsic incompatibility between the hydrophilic-layered silicate and hydrophobic polymer matrix [LeBaron et al., 1999]. Long-chain alkyl ammonium surfactants were usually employed to modify the MMT interlayer galleries through cation exchange reactions so as to weaken the interaction between adjacent layers and to enhance the compatibility/wettability of the MMT layer with the polymer matrix [Yu et al., 2004]. Preparation of organically modified MMT (OMMT) and the property of organic surfactant play a crucial role in the formation of the structure and morphology of PCNs [Zhang et al., 2003].

Usually, the dispersion of clay particles in a polymer matrix results in the formation of three types of composite materials [Giannelis et al., 1999]. The first type is conventional phase separated composites in which the polymer and the inorganic host remain immiscible resulting in poor mechanical properties of the composite material. The second type is intercalated polymer-clay nanocomposites, which are formed by the insertion of one or more molecular chains of polymer into the interlayer or gallery space. The last type is exfoliated or delaminated polymer-clay nanocomposites, which are formed when the clay nanolayers are individually dispersed in the continuous polymer matrix. Exfoliated polymer-clay nanocomposites are especially desirable for improved properties because of the large aspect ratio and homogeneous dispersion of clay and huge interfacial area (and consequently strong interaction) between polymer chains and clay nanolayers [Fu and Qutubuddin, 2001].

Nanocomposites based on polyamide 6/polypropylene (PA6/PP) blend have been studied extensively by many researchers. Tang et al. [2004] reported that maleic anhydride grafted polypropylene (PP-g-MA) was an effective compatibilizer for PP/PA6/MMT nanocomposites with PP dominant. Feng et al. [2004] showed that the addition of organoclay led to a reduction in dispersed particle size of PA6 in the PP/PA6 blend. Recently, PA6/PP/organoclay nanocomposites with PA6/PP (70/30 parts) were studied by previous researchers [Chow et al., 2003, 2004, 2005a, 2005b, 2005c; Wahit et al., 2005; Hassan et al., 2006]. Most of PA6/PP/organoclay nanocomposites were prepared using commercial organoclays. To our knowledge, preparation of PA6/PP nanocomposites using clay modification was still limited. In this study, sodium montmorillonite was modified using three different types of alkylammonium salts, i.e. dodecylamine, 12-aminolauric acid, and stearylamine. The research work presented in this thesis focuses on the effect of clay modification on the mechanical, thermal, and morphological properties of nanocomposites based on PA6/PP blend (70/30 parts). PA6/PP/organoclay nanocomposites were produced via melt compounding method (extrusion and injection molding). A PA6 dominant was chosen because of its good compatibility with the organoclay. As both PA6 and organoclay have polar characteristics, silicate layers of organoclay are easily exfoliated in the PA6 [Dasari et al., 2005]. PA6/clay nanocomposites have first been successfully synthesized by Usuki et al. [1993] and found that PA6/clay nanocomposites exhibited various superior properties such as high strength, high modulus, and high heat resistance compared to neat PA6. A minor portion of PP (30 wt %) was added into PA6 matrix with the aim of improving toughness, processability, dimension stability, and water barrier properties of PA6. Heino et al.

[1997] reported that the highest impact strength was achieved at the composition of PA6/PP (70/30) for PA6/PP blends.

## **1.2 Problem Statement**

In recent years, there has been increasing interest in the development of polymer blends based on PA6 and PP. PA6 is engineering plastic extensively used in the manufacture of automobile parts, engineering products and textile fibers because of their high mechanical strength and modulus and good processing ability. However, PA6 normally has a high affinity for water and its mechanical properties are often significantly affected by the absorption of water. It is also known to be a notch sensitive thermoplastic owing to a markedly lower resistance to crack propagation than to crack initiation. PP is commercial plastic which has good overall mechanical performance, good moisture resistance and low cost, but it shows relatively poor chemical and heat resistance. Thus, PA6 is frequently blended with the PP in order to improve mechanical properties, lower water absorption, and reduce materials cost [Zeng et al., 2002]. Unfortunately; these are incompatible polymers owing to different polarities and crystalline structure. It has been published well that compounding polymers with inorganic material including organoclay can improve the mechanical, barrier, and thermal properties of the resultant polymer composites [LeBaron et al., 1999].

Chow et al. [2004] reported that the enhancement in the mechanical properties of PA6/PP nanocomposites with the presence of organoclay was still limited. This is caused by the lack interaction between the organoclay and PP components and missing compatibility between the major and minor phases (i.e. PA6

and PP, respectively). Significant improvement in blend properties can usually be achieved by the addition of a suitable compatibilizer that was mostly polymer functionalized with maleic anhydride (MA). Maleic anhydride grafted polypropylene (PP-g-MA) and maleic anhydride grafted styrene-ethylene/butylene-styrene (SEBS-g-MA) were chosen because both of them have been found suitable to compatibilize the PA6/PP blends [Ide and Hasegawa, 1974; Sathe et al., 1996; González-Montiel et al., 1995a]. Ide and Hasegawa [1974] achieved compatibility in PP/PA6 blends using PP-g-MA as compatibilizer. Sathe et al. [1996] reported that the presence of PP-g-MA improved mechanical and thermal properties of PP/PA6 blends due to better adhesion between the two phases. According to González-Montiel et al. [1995a], SEBS-g-MA was found to serve both as a good compatibilizer and impact modifier arising from its elastomeric segments (ethylene/butylene). During a melt-mixing process, maleic anhydride groups of the functionalized polymers can react readily with the amine terminal groups of PA6, leading to the formation of copolymers which contribute to decrease the interfacial tension and to enhance phase dispersion and interfacial adhesion between PA6 and PP components [Zeng et al., 2002]. Accordingly, it may be expected that the mechanical and thermal properties of PA6/PP/organoclay nanocomposites could be further improved via the incorporation of these compatibilizers.

Clay minerals such as montmorillonite (MMT) exhibit many interesting structural features including exchangeable interlayer cations, hydroxyl groups on the edges of clay platelets, and a high aspect ratio and small dimensions of the individual layers. However, the pristine silicate surface is generally too hydrophilic to be compatible with most polymers. To render the hydrophobic clay surface, they are

intercalated with organic cations such as alkylammonium salt through an ion exchange reaction [Giannelis et al., 1999]. Generally, there are two objectives for clay modification before melt compounding [Yu et al., 2004]. The first is to weaken the polar interaction between adjacent MMT layers and increase the distances between MMT layers, which are a prerequisite for polymer macromolecules to intercalate into the MMT galleries. The second is to enhance the affinity/compatibility between polymer and MMT, which provides a driving force for polymers to migrate into the MMT galleries. According to Reichert et al. [2000], the formation of nanocomposites by means of melt compounding is strongly influenced by several vital factors such as type of alkylammonium, additive presents during clay modification, processing temperature, shear rates, type and content of compaibilizer, and polymer viscosity. They reported a gradual increase in tensile modulus with basal spacing, caused by the increase in the carbon number of the alkyl group. Wang et al. [2001b] reported that the exfoliation and intercalation behaviors depended on the chain length of organic modifier in the clay and the hydrophilicity of polyethylene grafted with maleic anhydride. According to Fornes et al. [2002], the larger initial interlayer spacing may lead to easier exfoliation since platelet-platelet attraction is reduced. It is implied that diffusion of polymer chains inside clay galleries is less hindered due to increased spacing and then lead to improved exfoliation and performance. In this study, sodium montmorillonite was modified with three different types of alkylammonium salts, namely dodecylamine, 12-aminolauric acid, and stearylamine. Commercial organoclay (Nanomer I.30TC) containing octadecylamine as organic modifier was also used in this study. The carbon number of alkyl group was C12 for both dodecylamine and 12-aminolauric acid, and C18 for both stearylamine and octadecylamine, respectively. Thus, it could

be expected that the montmorillonite modified with stearylamine and octadecylamine would have the larger initial interlayer spacing due to larger carbon number, better exfoliation, and then give better efficient reinforcement effect in the PA6/PP/organoclay nanocomposites than the montmorillonite modified with dodecylamine and 12-aminolauric acid. Further, the addition of compatibilizers (PP-g-MA and SEBS-g-MA) into the PA6/PP/organoclay nanocomposites should improve more exfoliation and the mechanical properties.

During the past several years, polymer nanocomposites have found an increasing number of applications in many structural automotive components, such as instrument panels, radiator fans, and electronic modules [Broge, 2000]. The principal reason for this increasing attention is the fact that polymer nanocomposites provide the enhanced stiffness, strength, and thermal stability at a relatively low cost. Most of these applications require good performance over a range of deformation rates. Hence, it has become important to know the effect of testing speed on the mechanical behavior of polymer nanocomposites. The primary objective of understanding the mechanical behavior at varying testing speeds is to assist the designer with reliable data relevant to practical applications. It is well known that the mechanical properties of most materials vary with the rate of loading and this effect is particularly evident in polymers [Askeland, 1996]. Studies on the effect of testing speed on mechanical properties of polymer nanocomposites have been done by several researchers. Shen et al. [2004] studied the effect of strain rate on surface deformation behavior of polyamide 66/organoclay nanocomposites by nanoindentation technique. They found that the hardness and plasticity index of PA66 and its nanocomposites were found to increase with strain rate. However, the elastic

modulus of the PA66 and its nanocomposites are shown to be insensitive to the strain rate as the motion of the amorphous population in the semi crystalline materials has been ‘locked’ at the temperature much lower than glass transition temperature ( $T_g$ ). Zhou et al. [2005] found that the elastic modulus and yield strength of increased with increasing testing speed for PP/clay nanocomposites. Very recently, Bao and Tjong [2008] investigated the effects of testing speeds and temperature on the mechanical properties of PP/multi-walled carbon nanotubes (MWNT) nanocomposites. They reported that the strength of PP/MWNT nanocomposites increased with increasing the testing speed but decreased with increasing the test temperature. So far, there exists no information available on the effect of testing speed on the mechanical properties of PA6/PP/organoclay nanocomposites. In the present work, the effect of testing speed on tensile property and fracture toughness of PA6/PP/organoclay nanocomposites will be investigated.

Polyamide 6 is sensitive to water due to the hydrogen-bond-forming ability of the amide groups. Water essentially replaces amide-amide-hydrogen bond with amide-water-hydrogen bond. Consequently, water absorption decreases with decreasing concentration of amide groups in the polymer backbone. Water acts as a plasticizer, which increases toughness and flexibility while reducing tensile strength and modulus [Ebewele, 1996]. In this work, a minor portion of a hydrophobic component (30 wt% PP) was incorporated into the PA6 matrix, aimed to increase the water resistance of PA6. Numerous researchers have reported that the PA6/organoclay nanocomposites showed less water absorption as compared with the pure PA6 matrix [Kojima et al., 1993a; Akkapeddi, 2000; Liu et al., 2003a; Mohanty and Nayak, 2007]. The improvement in water resistance of PA6/organoclay

nanocomposites could be attributed to the presence of immobilized and partially immobilized polymer in amorphous phase [Liu et al., 2003a; Mohanty and Nayak, 2007]. In addition, the rate of water absorption in PA6 nanocomposites is reduced compared to the unfilled polymer because of the impermeable silicate layers in the polymer. These layers increase the path-length for diffusion through the polymer [Vlasveld et al., 2005]. Chow et al. [2005a] reported that the presence of PP-g-MA in the PA6/PP/organoclay nanocomposites not only enhanced the resistance of the nanocomposites against direct water immersion but also improved the resistance of the composites against hygrothermal attack. Amine groups in the organoclay may react with amide groups of PA6 and PA6-g-PP copolymer via hydrogen bonding resulting in less possibility for the water molecules to interact with the octadecylamine. This may be attributed to possible sites for bonding of the octadecylamine already being occupied by either PA6 (amide group) and PP-g-MA (maleic anhydride group). Thus, it may be expected that the addition of compatibilizers (PP-g-MA and SEBS-g-MA) could improve the water resistance of the PA6/PP nanocomposites with various different types of clay modification.

### **1.3 Objectives of Study**

This study is concerned with PA6/PP/organoclay nanocomposites. The main objectives of this study are divided into the following categories:

- To explore the effect of organoclay loading on the mechanical, morphology, and thermal properties of PA6/PP blend.
- To evaluate the effect of clay modification and compatibilizers (PP-g-MA and SEBS-g-MA) on the mechanical, morphology, and thermal properties of PA6/PP/organoclay nanocomposites.
- To study the effect of testing speed on the mechanical and morphology behavior of PA6/PP/organoclay nanocomposites.
- To evaluate the water absorption behavior of PA6/PP/organoclay nanocomposites.

## **CHAPTER 2**

## LITERATURE REVIEW

### 2.1 Thermoplastics

Thermoplastics are resins that repeatedly soften when heated and harden when cooled. Many are soluble in specific solvents and burn to some degree. Compared with thermosets, thermoplastics generally offer higher impact strength, easier processing and better adaptability to complex designs [Rosato, 1997]. The thermoplastic can be divided into two classes, commodity plastics (i.e. polyethylene (PE), polypropylene (PP), and polystyrene (PS)), and engineering plastics (i.e. polyamide (PA), polyoxymethylene (POM), and polycarbonate (PC)).

#### 2.1.1 Polyamide 6 (PA6)

Nylon is a generic name of synthetic polyamides in which amide groups recur as integral parts of the main polymer chains. In 1935, nylon 6,6 (polyhexamethylene adipamide) is the nylon first prepared through condensation polymerization by W.H. Carothers. P. Schlack succeeded in preparing nylon 6 by heating  $\epsilon$ -caprolactam with water to height molecular. The large-scale production of nylon 6 was started by I.G. Farbenindustrie, which was largely used as bristles and filaments [Kim, 2000]. Nylons (polyamides) are characterized by the amide group ( $-\text{CONH}-$ ), which forms part of the polymer main chain (inter unit linkage). The amide groups are polar in nature and significantly affect the polymer properties. The polarity of these amide group allows for hydrogen bonding between chains, improving the inter chain attraction, and this gives polyamide polymers good mechanical properties [Baker and Mead, 2002]. However, the presence of amide groups in the polyamide leads to increase water absorption [Brydson, 1995].

In terms of chemical structure, polyamides may be divided into two basic types: those based on diamines and dibasic acids (A–A/B–B type); and those based on amino acids or lactams (A–B type). Polyamides are described by a numbering system that reflects the number of carbon atoms in the structural units [Ebewele, 1996]. A–A/B–B polyamides are designated by two numbers, with the first representing the number of carbon atoms in the diamine and the second referring to the total number of carbon atoms in the acid. Polyamide 6,6 (PA6,6) represents hexamethylene diamine and adipic acid. In addition, A–B type polyamides are designated by a single number. PA6 represents polycaprolactam [poly( $\omega$ -amino caproic acid)].

Among the polyamides, PA6,6 and PA6 are of the greatest commercial importance and most widely used because they offer a good balance of properties at an economic price [Ebewele, 1996]. PA6,6 is formed by the step-growth polymerization of hexamethylene diamine and adipic acid as shown in Figure 2.1. PA6,6 is characterized by a combination of high strength, elasticity, toughness, resistance to abrasion and organic solvent. PA6,6 has a moderately low specific gravity, 1.14 and its moisture resistance is fair. PA6 is made by ring-opening polymerization of  $\epsilon$ -caprolactam as shown in Figure 2.2. Both PA6,6 and PA6 physically differ in terms of melting point, glass transition temperature, crystallinity, and tensile modulus, among other things. PA66 has a melting point of 262°C, which is higher than that of PA6 at 225°C; its glass transition temperature is 65°C, versus 52°C for PA6; the crystal structure of PA66 is triclinic while PA6 has a monoclinic structure; and its tensile modulus is around 2.9 GPa, while it is a little lower for PA6. Some of these differences can be traced to the difference in symmetry of their repeat

units and to the difference in configuration of functional units at the chains ends. PA6 generally has one amine and one carboxylic acid group at the end of each chain; whereas, PA66 contains a mixture of chains that have only amines, only acid groups, or a combination of the two at their ends [Chavarria and Paul, 2004]. The most important application of polyamides is as fibers, which account for nearly 90% of the world production of all polyamides. For application in mechanical engineering includes gears, cams, bushes, bearings, and valve seats [Chanda and Roy, 1998].

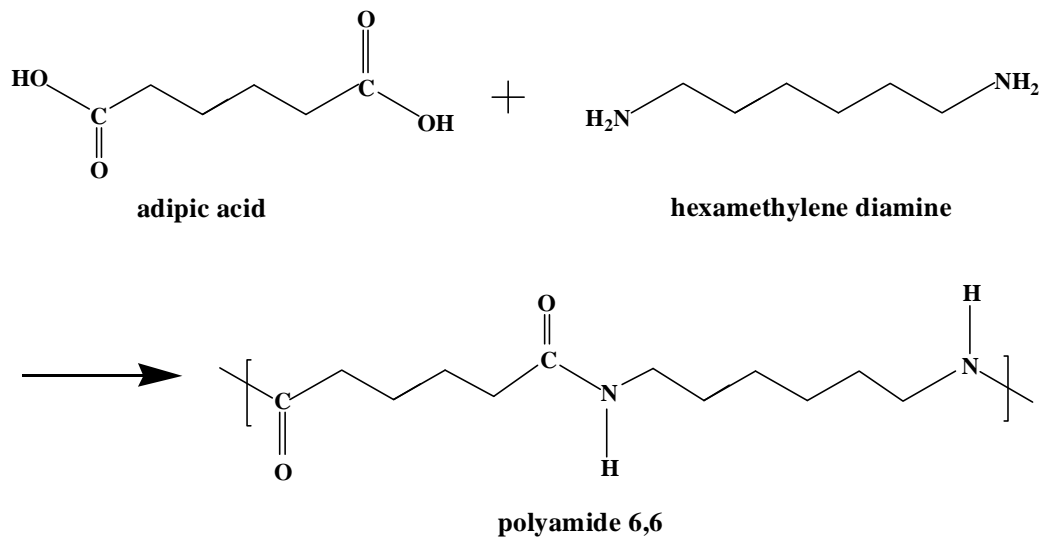


Figure 2.1: Synthesis of polyamide 6,6 [Painter and Coleman, 1994]

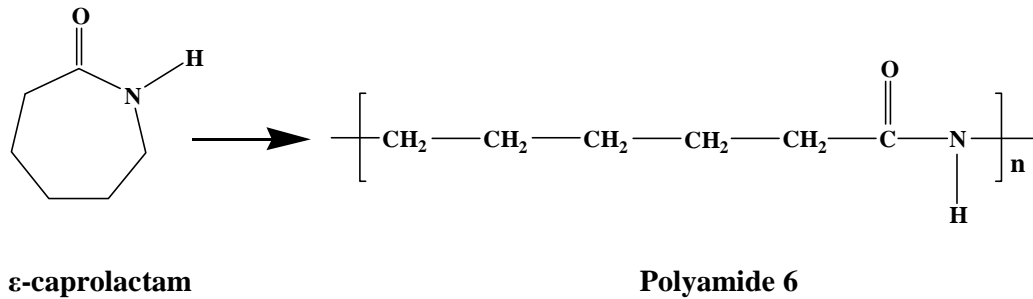


Figure 2.2: Typical ring-opening polymerization of caprolactam [Painter and Coleman, 1994]

### 2.1.2 Polypropylene (PP)

PP is the third-largest volume polyolefin and one of the major plastics worldwide [Ebewele, 1996]. In 1954, G. Natta of Milan following the work of K. Ziegler in Germany found that certain “Ziegler-Natta” catalyst were capable of producing high molecular weight polymers from propylene and many others olefins. The commercial PP was first introduced by Montecatini as Moplen in 1957 [Nicholson, 1991]. PP is a linear hydrocarbon polymer containing little or no unsaturation. PP and polyethylene (PE) have many similarities in their properties, particularly in their swelling and solution behavior and electrical properties. But, the many similarities the presence of a methyl group (-CH<sub>3</sub>) attached to alternate carbon atoms on the chain backbone can change the properties of the polymer in a number of ways, e.g. causing stiffening and rendering it less stable than PE with regards to oxidation [Brydson, 1995; Roff and Scott, 1971]. PP can be made from the monomer propylene by Ziegler–Natta polymerization and by metallocene catalysis polymerization of propylene to polypropylene. Figure 2.3 shows the polymerization of propylene to polypropylene.

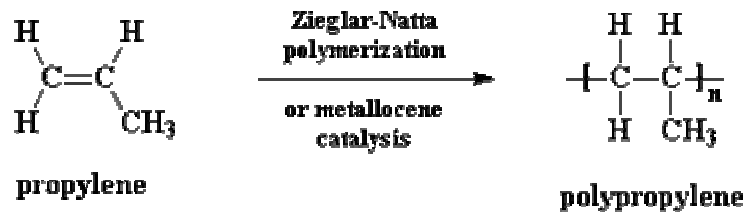


Figure 2.3: Polymerization of propylene to polypropylene [Baker and Mead, 2002]

PP can be made in isotactic (*i*-PP), syndiotactic (*s*-PP), and atactic (*a*-PP) forms. Isotactic PP shows a high degree of order with all the CH<sub>3</sub> groups along one side. Syndiotactic PP is a polypropylene with methyl groups alternating regularly from side to side. Atactic PP is rubbery, transparent material of limited commercial value; with methyl groups distributed at random side. Both isotactic and syndiotactic PP are highly crystalline: regularity of structure permits their molecules to fit together well. Commercially available PP is about 90 to 95 percent isotactic [Richardson and Lokensgard, 1997]. Isotactic polyethylene is highly crystalline with a melting point of 165 to 171°C. Because of its crystalline character, PP, like other crystalline polyolefin, is soluble only at elevated temperature. The crystallinity decreased with increasing temperature. The non-crystalline phase of PP will become glassy and brittle below glass transition temperature ( $T_g$ ), soft and rubbery above  $T_g$ , the embrittlement of isotactic PP as a whole at low temperature is a direct consequence of the glass transition of the non-crystalline phase [Frank, 1969].

PP is one of the lightest of the widely used commercial thermoplastics with a density in the range of 0.90-0.91 g/cm<sup>3</sup>. PP has excellent electrical and insulating properties, chemical inertness, and moisture resistance typical of nonpolar hydrocarbon polymers. It is resistant to a variety of chemicals at relatively high

temperatures and insoluble in practically all organic solvents at room temperature. PP is practically free from environmental stress cracking. PP is used in applications ranging from injection-molded and blow-molded products and fibers and filaments to films and extrusion coatings. Injection molding uses, which account for about half of PP produced, include applications in the automotive and appliance fields. PP can be designed with an integral hinge fabricated into products ranging from pillboxes to cabinet doors. Extruded polypropylene fibers are used in products such as yarn for carpets, woven and knitted fabrics, and upholstery fabrics [Ebewele, 1996].

## **2.2 Polymer Blends**

Polymer blends are a mixture of at least two polymers or copolymers [Utracki, 1990]. Polymer blending is one of the effective ways to obtain materials with specific properties. Blending not only can improve processability, mechanical and chemical properties but also the desired properties. There are several methods of blending, including mechanical, solution, latex, fine powder, as well as several variations known in the interpenetrating polymer network (IPN) technology. In the economic point of view, the mechanical blending predominates. According to Utracki [1998], polymer blend performance depends on the three factors; properties of ingredients, their content and morphology.

In recent years, there has been increasing interest in the development of polymer blends based on PA6 and PP. The reasons for blending PA6 with PP are, on the one hand, to improve particular properties of PA6 (e.g., toughness, moisture absorption, and processability) and, on the other, to improve the performance of PP (e.g., rigidity, thermal stability, and barrier properties to oxygen and solvents)

[Vocke et al., 1999]. Owing to its lack of polarity, PP is immiscible with PA6. Unfavorable interaction at the molecular level lead to high interfacial tension and make the melt mixing of the components difficult. This leads to an unstable morphology and poor interfacial adhesion, and the end result is blends with mechanical properties inferior to what would be expected by the additive mixing rule. Therefore, compatilizing agents have to be used to reduce the interfacial tension and to improve the adhesion between PA6 and PP [Piglowski et al., 2000]. Blends of PA6 with PP, when properly compatibilized, can potentially offer a wide range of desirable characteristics such as good mechanical properties, good chemical resistance, low water absorption, and reduced cost [González-Montiel et al., 1995a].

### **2.3 Compatibilization in Polymer Blends**

Polymer blending is economical route to getting new polymer materials at low cost and combining the performance of the corresponding neat polymers [Zeng et al., 2002]. Beside that, blends can be tailored to meet the requirements of specific applications. They can be developed much more quickly than new polymers and require much less capital investment. The properties of the blends are strongly depending on the compatibility of the system. However, most of the polymer blends are found to be incompatible. These incompatible blends are characterized by a two-phase morphology, narrow interphase, poor physical and chemical interactions across the phase boundaries, and poor mechanical properties [George et al., 1995]. These problems can be alleviated by the addition third component into the incompatible polymer blends to enhance the degree of compatibility between the constituent components [Bonner and Hope, 1993]. The third component is called compatibilizer. Compatibilizers are macromolecular species exhibiting interfacial activities in

heterogeneous polymer blends. The role of compatibilizer is similar to that of emulsifiers in classical emulsion technology. The compatibilizer should migrate to the interface, reducing the interfacial tension coefficient, reducing the dispersed phase dimensions, stabilizing the blend morphology and enhancing the adhesion between phases in the solid state [Utracki, 1998].

There are three famous methods of compatibilisation of polymer blends, namely the addition of block and grafted copolymer, the addition of functional polymers, and reactive blending. The addition of block and grafted copolymer is one of an effective way to compatibilize the immiscible blends. The block and grafted copolymers containing segments chemically identical to the blend components are obvious choices as compatibilizer, given that miscibility between the copolymers segments and the corresponding blend components is assured. The addition of functional polymers, a polymer chemically identical to one of the blend components is modified to contain functional or reactive units [Bonner and Hope, 1993]. These functional units have some affinity for the second blend component, which have the ability to chemically react with the second blend component. For example, the grafting of maleic anhydride or similar compounds to polyolefins, result in the formation of pendant carboxyl group which have the ability to form a chemical bridge with polyamides via their terminal amine groups. The reactive blending is a new technical method of producing compatible polymers blends. This method is relied on the in situ formation of copolymers or interacting polymers. This differs from other compatibilisation routes in that blend components themselves are either chosen or modified so that reaction occurs during melt mixing, with no need for addition of a separate compatibilizer [Bonner and Hope, 1993]. In some cases, the

reaction may be produced by adding a monomeric ingredient, which can serve as a catalyst, free radical initiator and co reactant in the reaction between the two polymers [Deanin and Manion, 1999]. Beside that, the reaction can also be produced by the treatment conditions. For example, Oh et al. [2003] have reported the preparation of in situ compatibilisation PP/natural rubber blends via twin-screw extruder and ultrasonically treated during the extrusion process. The improved interfacial adhesion, morphology and mechanical properties of the blends are believed to be due to the formation of in situ copolymer at the interface of two immiscible polymers caused by an ultrasonic treatment without the use of any chemicals. Table 2.1 lists the polymer blends with compatibilizers.

Table 2.1: Polymer blends with compatibilizers

Polymer blends	Compatibilizers	References
LDPE/PA6	PE-PEO	Halldén et al., 2001
	PE-g-MA	Jiang et al., 2003
PC/PA6	SEBS-g-MA	Lee et al., 1999
PP/PS	SBS	Waldman and De Paoli, 2008
PBT/PA6	SMA	Shu-ha et al., 2007
PP/PA6	PP-g-MA	Sathe et al., 1996
	POE-g-MA	Bai et al., 2004
	SEBS-g-MA; EPR-g-MA	González-Montiel et al., 1995a
	PP-g-MA-co-POP	Tseng et al., 2001

### 2.3.1 Maleic Anhydride Grafted Polypropylene (PP-g-MA)

A commonly used method for inducing compatibility between polyamide and polyolefin (i.e. polypropylene) is by chemical modification of the polyolefin to contain pendent carboxyl groups, often by grafting with maleic anhydride or similar compounds, which form chemical linkages to the polyamide via the terminal amine groups [Bonner and Hope, 1993]. For many years, following the early pioneering advances by Ide and Hasagawa [1974], maleic anhydride grafted polypropylene (PP-

g-MA) has been used extensively for compatibilization of PP and PA6. In the melt, the maleic anhydride groups can easily react with the amine end groups of PA6 to form block or graft copolymers. These resulting copolymers efficiently reduce the interfacial tension between PP and PA6, thus, also reducing the size of dispersed PA6 phase and enhancing the mechanical properties of the blends. Sathe et al. [1996] reported that PA6/PP blends containing PP-g-MA showed more regular and finer dispersion, different dynamic properties, and improved mechanical properties due to the better adhesion between the two phases. In addition, the addition of PP-g-MA into the PA6/PP blends also lower MFI and water absorption properties due to the formation of PP-g-PA6 copolymer during melt mixing. According to Marco et al. [1997], the presence of PP-g-MA in the PA6/PP leads to a reduction in the crystallinity of the polyamide 6 and in its rate of crystallization, due to the diluent effect of the polypropylene. A similar compatibilization effect of PP-g-MA in the PP/PA6 blends was also reported by Tseng et al. [2001], Roeder et al. [2002], and Zeng et al. [2002]. Roeder et al. [2002] found that the compatibilized PP/PA6 blends absorbed less water than corresponding uncompatibilized systems, probably related to the fewer N-H groups due to imide linkage formation. The compatibilized blends can form a hydrogen bond that reduces the interfacial tension and the possibility of forming capillaries between domains and matrix. Then, the interfacial layer formed with the addition of PP-g-MA increases the adhesion between the phases and reduces voids and water uptake.

### **2.3.2 Maleic Anhydride Grafted Styrene-Ethylene/Butylene-Styrene (SEBS-g-MA)**

SEBS is a triblock (ABA-type) thermoplastic elastomer that combines the melt processability of polystyrene (PS) and the elastomeric properties of poly(ethylene/butylene) [Jose et al., 2006]. SEBS-g-MA has been known to be good impact modifiers and compatibilizers for PA6/PP blends [González-Montiel et al., 1995a and 1995b; Ohlsson et al., 1998; Kim et al., 1998]. The maleic anhydride groups grafted to the rubber react with the amine end-group of PA6, forming a SEBS-g-PA6 copolymer that helps to disperse the rubber in the PA6 matrix and to strengthen the PA6/PP interface [González-Montiel et al., 1995b]. According to González-Montiel et al. [1995a and 1995b], there are many variables that may affect the toughness of PA6/PP blends: the ratio of PA6 to PP, the volume fraction of the rubber, the molecular weights of the PA6 and PP, the composition and degree of functionality of the rubber and the degree of functionality of the PP. Toughness was greatest for these blends when the PA6 phase was continuous and the rubber and PP were well dispersed in it. The molecular weights of nylon 6 and polypropylene affect the toughness of the blends through changes in morphology in response to the melt viscosity of these components. By simply adjusting component melt viscosities, nylon 6 or polypropylene can be made the continuous phase. Molecular weight also influences the intrinsic ductility of the pure components. González-Montiel et al. [1995c] reported that the mechanism of toughening in rubber-modified PA6/PP blends was cavitation of the rubber dispersed as particles in the PA6 and at the PA6/PP interface. The structure of the rubber modifier and its particle size are factors that contribute to the differences observed in the extent of cavitation of nylon 6/PP blends modified with SEBS-g-MA or EPR-g-MA. Kim et al. [1998] also studied the

micromechanical deformation process in toughened PP/PA6/SEBS-g-MA blends and observed that the blend morphology, that is, the rubber dispersion, changed significantly with an increasing volume fraction of SEBS-g-MA. In addition, the major toughening mechanism is the fibrillized cavitation process, and the main energy dissipation during deformation is shear yielding of matrix material triggered by irreversible plastic growth of microvoids caused by the fibrillized cavitation process.

## **2.4 Thermoplastic Composites**

Composite is defined as a material consisting of two or more distinct phases with an interface between them. This definition is basically used for materials containing reinforcements characterized by a high aspect ratio, as in the case for fibers, platelets and flakes. The incorporation of these materials into thermoplastics matrices results in improved, but possibly anisotropic, mechanical and thermal properties. The role of the matrix, reinforcement and interface in composites are well defined. The matrix is responsible for transferring the load from the matrix to the reinforcement, for distributing the stress among the reinforcement from environmental attack, and for positioning the reinforcing material. Meanwhile, the task of the reinforcement is to carry the load, due to its higher stiffness and strength compared with that matrix. The interface (for two dimensions) or the interphase (for three dimensions) is a negligible or finite thin layer with its own properties, and its role is stress transfer from the matrix to the reinforcement [Karger-Kocsis, 2000]. The mechanical performance of reinforced thermoplastic blends is affected by several factors, including blend composition and morphology, type and amount of

the reinforcement, interface and interphase between matrix and reinforcement, processing methods and testing conditions.

## **2.5 Polymer Nanocomposites**

Polymer nanocomposites are a new class of composites, which are particle-filled polymers for which at least one dimension of the dispersed particles is in the nanometer range. One can distinguish three types of nanocomposites, depending on how many dimensions of the dispersed particles are in the nanometer range. When the three dimensions are in the order of nanometers, we are dealing with isodimensional nanoparticles, such as spherical silica nanoparticles obtained by in situ sol gel methods. When two dimensions are in the nanometer scale and the third is larger, forming an elongated structure, we speak about nanotubes or whiskers as, for example, carbon nanotubes or cellulose whiskers which are extensively studied as reinforcing nanofillers yielding materials with exceptional properties. The third type of nanocomposites is characterized by only one dimension in the nanometer range. In this case the filler is present in the form of sheets of one to a few nanometer thick to hundreds to thousands nanometers long. This family of composites can be gathered under the name of polymer-layered silicate nanocomposites. These materials are almost exclusively obtained by the intercalation of the polymer (or a monomer subsequently polymerized) inside the galleries of layered host crystals. There is a wide variety of both synthetic and natural crystalline fillers such as graphite, metal chalcogenides, carbon oxides, metal phosphates, layered double hydroxides, clays and layered silicates. Among all the potential nanocomposite precursors, those based on clay and layered silicates have been more widely investigated probably because the starting clay materials are easily available and their potential intercalation ability.

Owing to the nanometer-size particles obtained by dispersion, these nanocomposites exhibit markedly improved mechanical, thermal, optical and physico-chemical properties when compared with the pure polymer or conventional (microscale) composites [Alexandre and Dubois, 2000]. Polymer layered silicate nanocomposites are a hybrid between an organic phase (the polymer) and an inorganic phase (the silicate). The choice of the silicate determines the nanoscopic dispersion typical of nanocomposites. The silicates employed belong to the family of layered silicates also known as phyllosilicates, such as mica, talc, montmorillonite, vermiculite, hectorite, saponite, etc [Zanetti et al., 2000].

## 2.6 Filler

Materials which are added to a polymer matrix to improve a property or properties fall in the category of either reinforcement or filler. Generally, a material which raises the mechanical properties of a composite over that of the base resin is called a reinforcing material. They are usually fibrous in nature. Mechanical properties affected are parameters such as Young's modulus, tensile strength, and toughness. Fillers are those materials which are added as inert extender and are usually spherical in form. Table 2.2 shows various fillers that classified according to their forms.

Table 2.2: Forms of various fillers [Charrier, 1990]

Spherical	Fiber	Platelet
Calcium carbonate	Glass fiber	Kaolin
Silica	Carbon fiber	Talc
Carbon black	Graphite fiber	Clay
Feldspar	Metal fiber	Wollastonite
Solid glass sphere (bead)	Asbestos	Muscovite
Aluminum trihydrate	Whisker	Phlogopite
Calcium sulfate solid	Cellulose	